



Broken phase of parity-time symmetry enables efficient superluminal pulse transmission

LI-TING WU,¹ XIN-ZHE ZHANG,² MING KANG,³ 
TIAN-JING GUO,^{4,5}  AND JING CHEN^{2,*} 

¹School of Information and Communication Engineering, Nanjing Institute of Technology, Nanjing 211167, China

²School of Physics, Nankai University, Tianjin 300071, China

³College of Physics and Materials Science, Tianjin Normal University, Tianjin 300387, China

⁴Institute of Space Science and Technology, Nanchang University, Nanchang 330031, China

⁵tianjing@ncu.edu.cn

*jchen4@nankai.edu.cn

Abstract: Parity-time (\mathcal{PT}) symmetric Bragg gratings (PTBGs) exhibit unique band characteristics compared to their traditional counterparts. Notably, when the \mathcal{PT} symmetry is broken, the initial bandgap closes, and the upper and lower branches coalesce. We demonstrate that this believed to be novel band dispersion supports fast light, also known as the optical superluminality. A light pulse can propagate through a fiber PTBG with broken \mathcal{PT} symmetry, achieving high transmission efficiency (comparable to, and even exceeding, unity) while maintaining its Gaussian shape. This effect offers a significant advantage over superluminal tunneling, where the transmission coefficient is typically very small. We also analyze the transmission of optical precursors and show that they cannot be superluminal, consistent with the principle of causality. This work presents a mechanism for realizing superluminality with some possible applications and underscores the vast potential of non-Hermitian optics.

© 2024 Optica Publishing Group under the terms of the [Optica Open Access Publishing Agreement](#)

1. Introduction

Over the past decade, the concept of parity-time (\mathcal{PT}) symmetry [1–4] has gained significant attention within the physics community. A \mathcal{PT} system is characterized by spatially distributed gain and loss, making it an open system that does not conserve energy. This unique property has led to the proposal and demonstration of various interesting phenomena and effects that cannot exist in traditional closed systems [5–9]. The study of \mathcal{PT} symmetry has opened up new avenues for exploring the behavior of open systems and developing new technologies for manipulating light and matter.

The phases of \mathcal{PT} systems can be categorized into three types [1–4]. The phase characterized by real eigenvalues is termed the exact \mathcal{PT} phase. If any eigenvalue becomes complex, the \mathcal{PT} symmetry is said to be broken. The transition point separating the exact and broken \mathcal{PT} phases is known as the exceptional point (EP), where the quantum space collapses, and some real eigen-solutions coalesce. Most research on \mathcal{PT} symmetry has focused on EPs and the exact \mathcal{PT} phase. In the broken \mathcal{PT} phase, because complex eigenvalues typically represent decaying and growing modes, studies have primarily concentrated on the performance of lasing or coherent absorption in this regime, see [1,2] and references therein.

This article highlights a unique property of systems exhibiting broken \mathcal{PT} symmetry: their potential to enable efficient superluminal optical pulse transmission. We focus on \mathcal{PT} -symmetric Bragg gratings (PTBGs) in optical fibers [10–19] and demonstrate how a PTBG operating in the broken \mathcal{PT} phase can achieve this phenomenon. Superluminality, the seemingly paradoxical ability to exceed the speed of light has long intrigued physicists due to its apparent violation of Einstein's theory of special relativity and the principle of causality [20–22]. In classic closed

systems, superluminal behavior can be observed during tunneling through opaque barriers, such as traditional Bragg gratings [22–27]. However, the extremely low tunneling coefficients in such scenarios limit the practical applications of this effect. We show that introducing broken \mathcal{PT} symmetry can close the bandgap in PTBGs, leading to a dispersion relation with a slope greater than the speed of light c/n_b , where n_b is the index of refraction of the fiber. This enables efficient superluminal transmission of optical pulses, distinct from the tunneling phenomena. Additionally, we analyze the transmission of optical precursors [28–30] and demonstrate that their propagation speed remains c/n_b , consistent with the principle of causality regarding the transmission of signal (message or information). This work reveals a mechanism for achieving superluminality with some potential applications, contributing to the burgeoning field of non-Hermitian physics.

2. Method and analysis

2.1. Photonic band structure

Let us consider the fiber PTBG shown in Fig. 1, in which fields propagate along the x direction. The background medium of the fiber has a real refractive index of $n_b = 1.5$. A section of the fiber is imprinted with a perturbation of complex refractive index Δn so that $n(x) = n_b + \Delta n(x)$. Here we assume that the perturbation Δn is \mathcal{PT} symmetric. Within the unit cell of $-2d < x < 2d$, we can define 4 layers, where

$$\Delta n(x) = \begin{cases} +m(1 + j\delta), & -2d < x < -d, \text{ (layer - A)} \\ -m(1 - j\delta), & -d < x < 0, \text{ (layer - B)} \\ -m(1 + j\delta), & 0 < x < d, \text{ (layer - C)} \\ +m(1 - j\delta), & d < x < 2d, \text{ (layer - D)} \end{cases} \quad (1)$$

This definition of a unit cell implies that the refractive index perturbation satisfies the \mathcal{PT} -symmetry condition $\Delta n(-x) = \Delta n(x)^*$. Here, m (equal to 0.1) denotes the amplitude of modulation in the real part of the refractive index (n_r), while $m\delta$ represents the amplitude of modulation in the imaginary part (n_i). Parameter δ represents the strength of the \mathcal{PT} symmetry. The perturbation Δn exhibits periodicity with a period L equal to $4d$, where d is the thickness of each layer. It's important to note that the classification of Δn is not absolute. Shifting the unit cell by a distance d alters the layer sequence within the unit cell from $ABCD$ to $BCDA$. Consequently, if we re-define $x = 0$ as the interface between layers C and D , the refractive index perturbation within the $BCDA$ unit cell now obeys the relationship $\Delta n(-x) = -\Delta n(x)^*$. This specific symmetry condition is referred to as anti- \mathcal{PT} symmetry [31–33].

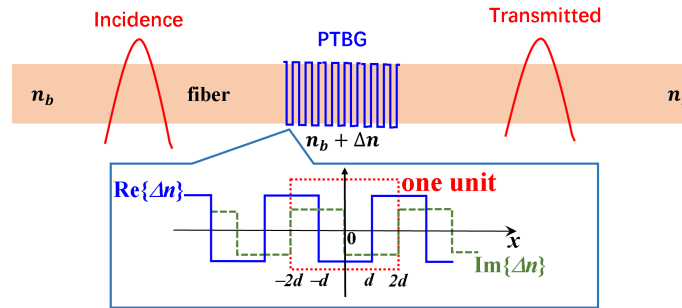


Fig. 1. Schematic of the PTBG configuration under investigation.

Considering the layered configuration of PTBGs shown in Fig. 1, with the step-like modulations in both n_r and n_i given by Eq. (1), we propose to use the semi-analytical approach of the transfer

matrix method (TMM) [5,8,10,16,19] to study the photonic band structure and the transmission properties of the fiber PTBGs. We first calculate the dispersion relation (ω, K) of PTBGs, where K is the Bloch wavevector. Although the emphasis of the present article is on the broken phase, to clearly demonstrate the novel dispersion of PTBG for superluminal light, we also show the scenario of an exact \mathcal{PT} phase at $\delta = 0.8$ in Fig. 2(a). In the exact \mathcal{PT} phase, a nonzero band gap around the Bragg frequency $\omega_{PBG} = c\pi/(Ln_b) = 0.667c\pi/L$ is open. This band gap can be referred as the ω gap [34,35], around which the group velocity, given by $v_g = \partial\omega/\partial K$, is smaller than c/n_b . This effect is a well-documented mechanism for realizing slow light or high density of states. Within the ω gap, no propagation mode is permitted, and the superluminal tunneling of it has been studied in the Refs. [19,22–27]. When the magnitude of δ increases and passes the EP around 1 [19], the \mathcal{PT} phase is broken. The ω gap is now closed. The upper and lower branches do not reach the Brillouin zone edge at $K_{BZ} = \pi/L$. Instead, they approach each other and connect smoothly at K_{EP} , which satisfies $K_{EP} < K_{BZ}$. The region between K_{EP} and K_{BZ} possesses complex K values due to the broken \mathcal{PT} phase [18,19]. We can refer to this gap as the K gap, similar to that in photonic time crystals [35]. The K gap is not the focus of this article because the external incident pulses from the input region possess real- ω harmonic components, which should mainly excite the modes in the gapless dispersion (ω, K) of the broken \mathcal{PT} phase. Focusing on the gapless dispersion (outside the K gap) shown in Fig. 2, we can see the arc of ω versus K evidently produces superluminality (or fast light) with $v_g > c/n_b$, as shown by the blue circles in Fig. 2(b). The existence of this fast-light dispersion, which ranges continuously across ω_{PBG} , is a key emphasis of this article.

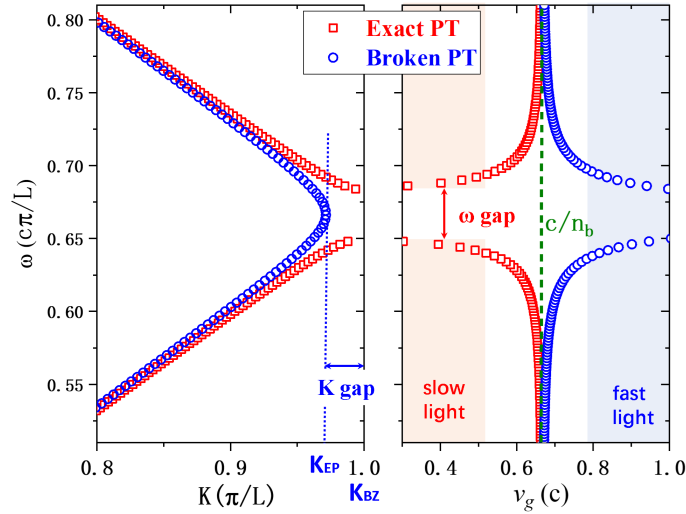


Fig. 2. Dispersion and group velocities at exact ($\delta = 0.8$, red squares) and broken ($\delta = 1.2$, blue circles) \mathcal{PT} phases, respectively.

When an optical pulse enters from the input region, its spectrum comprises various harmonic components, each with a distinct real angular frequency ω . Employing the TMM method allows us to determine the complex amplitudes of both forward and backward propagating waves for each harmonic component. These waves exhibit phases of $\exp[-jn(x)kx + j\omega t]$ and $\exp[jn(x)kx + j\omega t]$ respectively, where $k = \omega/c$ represents the real wave-number in free space. Figure 2 illustrates that despite the complex nature of the wave-vector $n(x)k$ within each layer (due to the complex refractive index $n(x)$), the Bloch mode of the periodic structure remains harmonic, characterized by a real Bloch wavevector K . However, it's important to note that Bloch's theorem strictly applies to infinitely long structures. In our scenario, both the input and output regions consist of uniform

fiber, while the PTBG section itself has a finite length. Consequently, the transmission spectra may exhibit features that deviate from the predictions of Bloch's theorem. To demonstrate the potential of the broken \mathcal{PT} phase for field manipulation, we investigate the transmission spectra and the corresponding phase gradient of a 100-period fiber PTBG by using TMM. The phase gradient τ_{gt} , which is also termed the group delay of transmission [19], is defined as the derivative of the transmission phase ϕ_t with respect to angular frequency, i.e., $\tau_{gt} = \partial\phi_t/\partial\omega$, where the complex transmission coefficient is defined by $t_{PTBG} = |t_{PTBG}| \exp(-j\phi_t)$. Transmittance (T) is the squared magnitude of the transmission coefficient, $T = |t_{PTBG}|^2$. To ensure comparability with conventional fiber Bragg gratings, we require the structure to function as a Bragg grating when the strength of the \mathcal{PT} symmetry (δ) is zero. Therefore, we modify the unit cell to a *DABC* sequence by shifting the original one by a quarter period. This modification preserves the dispersion relation (ω, K) while ensuring consistent transmission characteristics between the two unit cell definitions, as verified through our calculations discussed at the end of this article.

Figure 3 illustrates the transmission characteristics of PTBGs in the broken \mathcal{PT} phase when $\delta = 1.2$. The inset also displays the results in the exact \mathcal{PT} phase at $\delta = 0.8$. When the \mathcal{PT} phase is conserved, a tunneling region with nearly zero transmittance T around ω_{PBG} is observed, indicating the existence of a ω gap. However, when the \mathcal{PT} phase is broken, the ω gap closes, resulting in effective transmission. In this case, the transmittance T around ω_{PBG} exceeds one. The non-conservation of energy can be attributed to the non-Hermitian nature of PTBGs and the limited length of PTBGs, which violates the strict requirements of Bloch's theorem. The phase gradient τ_{gt} also reaches an extreme low value at ω_{PBG} . Although similar to that of the exact \mathcal{PT} phase, τ_{gt} can be smaller than zero at ω_{PBG} in the broken \mathcal{PT} phase, which is indicative of the fast-light dispersion shown in Fig. 2. Below, we will demonstrate that this \mathcal{PT} phase transition and the non-uniform T can still facilitate efficient transmission (no longer tunneling) of optical pulses while preserving their shapes.

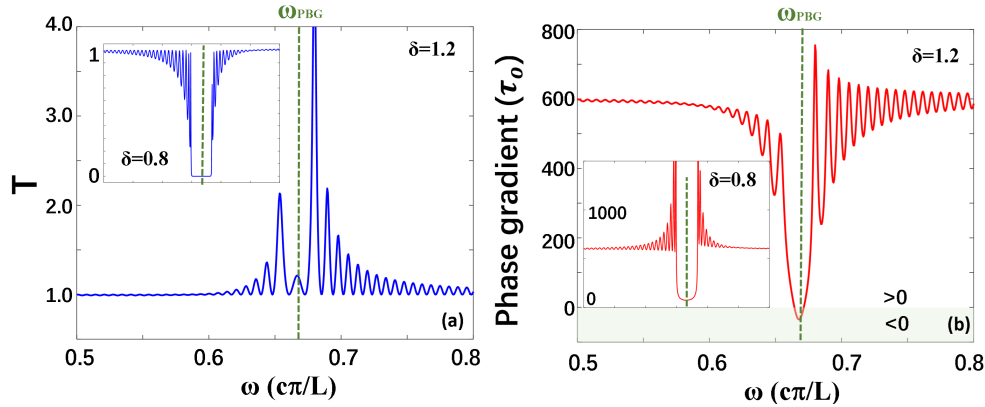


Fig. 3. (a) Transmittance and (b) the phase gradient versus ω when $\delta = 1.2$. Inset shows the results of $\delta = 0.8$. The unit of time τ_0 equals d/c .

2.2. Superluminal pulse transmission

The high transmittance and the fast-light dispersion would help to realize efficient superluminal transmission. To prove this effect, we use TMM to simulate the transmission of an optical pulse in the fiber PTBG. The incident field E_i is assumed to have a Gaussian profile in the x direction, and the central frequency is the Bragg one at ω_{PBG} (corresponding to a wavevector k of ω_{PBG}/c

in free space), that

$$E_i(x) = E_0 \exp \left[-\frac{(x - x_0)^2}{w_0^2} \right] \exp \left(-j \frac{n_b \omega_{PBG}}{c} x \right). \quad (2)$$

The waist w_0 of the pulse should be comparable to, or even larger than, the thickness of PTBGs. The initial position of the incident pulse is denoted as x_0 , and the origin of the coordinate system, $x = 0$, is set at the input interface of the fiber PTBG.

The incident pulse can be expressed as a Fourier series of $E_i = \sum_k E_k \exp(-jn_b kx)$. First, we use discrete Fourier expansion to find the spectrum of the incident pulse. Then, for each component E_k , we calculate the complex scattering coefficients in each layer (t_k for the forward wave and r_k for the backward wave) as well as in the input and output regions using TMM. At a given time delay t , the scattered field is reconstructed using the inverse discrete Fourier expansion. For example, consider layer A, where the complex field components at the input interface at x_A are $t_k^A E_k$ and $r_k^A E_k$. At time t , the complex field is given by $E_t^A(x) = \sum_k E_k \{ t_k^A \exp[-jn_A k(x - x_A)] + r_k^A \exp[jn_A k(x - x_A)] \} \exp(j\omega t)$ where $\omega = ck$.

Figure 4 illustrates the intensity distribution ($I = |E|^2$, normalized by $I_0 = |E_0|^2$) at various time delays within the structure with $x_0 = -550d$. The parameters used here are consistent with those in Figs. 2 and 3. The waist of the incident pulse, w_0 , is set to $240d$, which is comparable to the total thickness of the PTBG structure ($400d$). The blue dashed pulse serves as a reference, indicating the pulse's position and shape if it were to propagate directly through the fiber without interacting with the PTBG structure. As the pulse approaches and enters the PTBG structure, we observe the excitation of various harmonic modes within the structure, leading to interference patterns. When the time delay is sufficiently large (e.g., $> 1300\tau$), a transmitted pulse emerges on the other side of the PTBG. It's important to highlight that, unlike tunneling phenomena characterized by weak amplitudes, the transmitted pulse in this broken \mathcal{PT} -symmetric phase exhibits a comparable, and even larger, magnitude compared to the reference pulse. Moreover, the transmitted pulse retains its Gaussian shape and demonstrates a significant spatial advancement compared to the reference pulse, indicating superluminal transmission. The spatial advancement, denoted as Δ (as defined in Fig. 5), can reach up to $380d$ for the specific case presented in Fig. 4.

The efficient superluminal pulse transmission is sensitive to the waist w_0 of the pulse. On one hand, a larger w_0 can lead to a greater spatial advance Δ because the spectrum of the incident pulse, with a smaller broadening of $\delta\omega = c\delta k/n_b = c\hbar/2n_b w_0$, can be well situated inside the fast-light region. On the other hand, a large w_0 reduces the bit rate for potential communication applications, as discussed in the context of the buffer application of slow light [36]. To achieve high-bit-rate transmission, w_0 should be kept as small as possible. A smaller w_0 is associated with a larger $\delta\omega$, and the spectrum of the incident pulse might extend into the luminal region with $v_g = c/n_b$, thereby compromising the superluminal transmission. To demonstrate the trade-off between w_0 and Δ , we calculate the transmission of the pulse at various w_0 values. As shown in Fig. 5, when w_0 is larger than the previously discussed value, such as $w_0 = 400d$, the superluminal feature can still be observed. The spatial shift Δ saturates at $415d$ when w_0 exceeds $600d$. For short pulses with significantly smaller w_0 , for example, $200d$, the advance Δ in the pulse peak cannot be distinguished because the pulse undergoes multiple reflections inside the PTBG, resulting in a series of transmitted pulses. Similar results are found in the subsequent study on optical precursors.

It's crucial to emphasize that the observed superluminal transmission is intricately linked to the specific dispersion characteristics of the broken \mathcal{PT} -symmetric structure around its resonant frequency, ω_{PBG} . If the central frequency of the incident pulse is shifted away from ω_{PBG} , the group velocity predicted by the dispersion curve (as shown in Fig. 2) approaches the speed of light in the background medium (c/n_b). This implies that the pulse would experience neither a delay nor an advancement. Our TMM simulations (not included here) have validated this phenomenon.

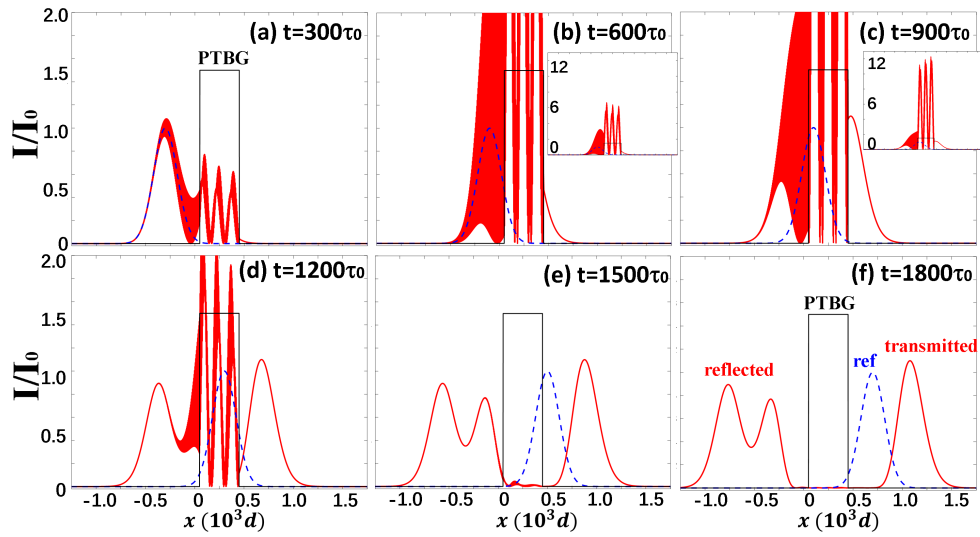


Fig. 4. Distributions of field intensity I/I_0 at different time delays, where $\tau_0 = d/c$. The blue dashed pulse represents the signal when it is directly transmitted through the fiber without the PTBG structure, and it is used as a reference. The insets in (b) and (c) show the global view of I/I_0 . The maximum value of I/I_0 is greater than 12 in (c).

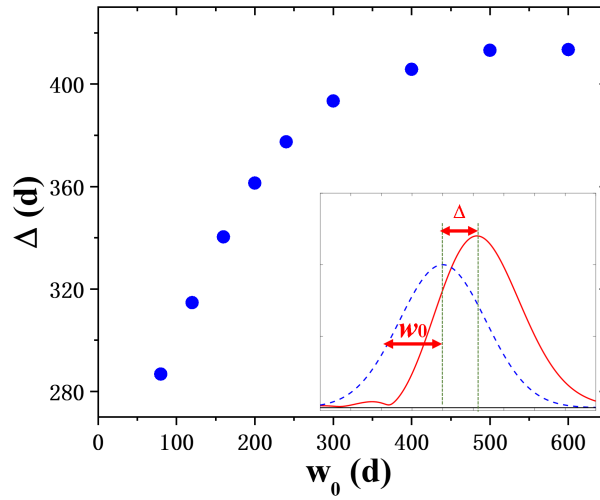


Fig. 5. The dependence of the spatial shift Δ versus the width w_0 of incidence.

2.3. Precursors are not superluminal

A long-standing debate on superluminality centers around whether it violates Einstein's theory of special relativity and the principle of causality, which states that the speed of any signal cannot exceed the speed of light. Various solutions to this paradox have been proposed. For example, in the case of superluminal tunneling, it is argued that since most of the energy is reflected, superluminal tunneling cannot effectively transport a signal [22]. For gain media, the paradox is explained using precursors, which are sharp singularity jumps in the pulse; since the signal cannot be predicted and cannot be expressed by any analytical mathematical formula [28–30]. In

open systems, such as time-varying photonic crystals, superluminality can be explained by the fact that energy is not conserved [35].

The fiber PTBGs discussed here are also open systems, meaning that energy is not conserved within them. However, we still aim to examine the mechanism of precursors in this article. Since a signal (or information) is inherently unpredictable, the Gaussian function used in Eq. (1) cannot represent a signal, as it is analytical for all values of x (from $-\infty$ to $+\infty$) and its position at a given time delay can be predicted if a distant observer can detect the local wave function from the signal. This predictability is why scientists have suggested that the simplest signal is the one in which the field is initially zero and then suddenly turns on to a finite value (or vice versa), which is commonly referred to as a step-modulated pulse [28–30]. These step-modulated pulse fronts can be considered as the optical precursors.

The precursors are random signals in the form of a δ function. To mimic a precursor, we start with E_i as given in Eq. (1) and assume that the leading edge is cut off to create a step-like front, that

$$E_i(x) = E_0 \exp\left(-j \frac{n_b \omega_{PBG}}{c} x\right) \begin{cases} \exp\left[-\frac{(x-x_0)^2}{w_0^2}\right], & x < x_0 \\ 0, & x > x_0 \end{cases} \quad (3)$$

Figure 6 illustrates the distribution of the field at various time delays. Notably, the transmitted pulse shape exhibits significant distortion compared to the reference. This distortion stems from the broadened spectrum of the precursor, primarily attributed to the step-modulated front. Consequently, the pulse undergoes multiple reflections within the PTBG, resulting in the splitting of the transmitted pulse into multiple peaks. Despite the superluminality of the main transmitted pulse, a step-shaped precursor remains observable and aligns precisely with the precursor on the reference. This observation confirms that the precursors propagate still at the speed of light in the fiber (c/n_b), reinforcing the principle that the signal cannot exceed the speed of light. This simulation agrees well with existing literature on precursors transmitted or tunneled through gain media or opaque barriers [28–30]. It further substantiates the interpretation of the precursor as the carrier of signal or information in physics, demonstrating its adherence to the principles of causality.

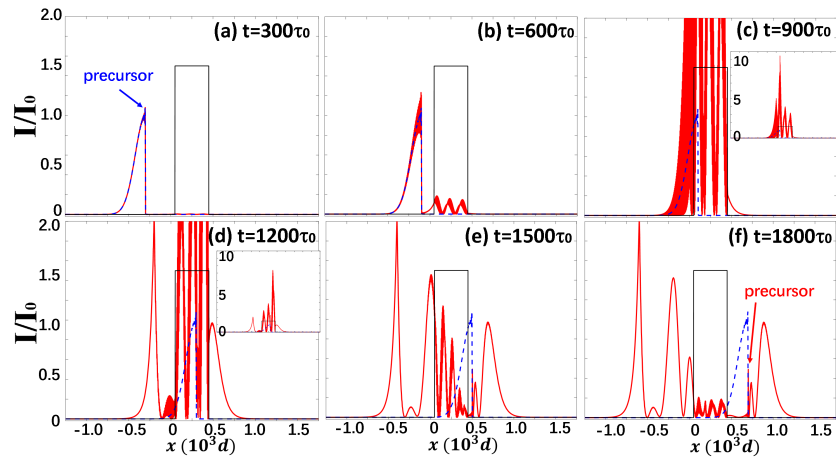


Fig. 6. Distributions of transmitted and reflected pulse for precursors at different time delays. Blue dashed pulse is the reference. The insets in (c) and (d) show the global view of I/I_0 . The maximum value of I/I_0 is greater than 10 in (c).

3. Discussion

Each unit of PTBG comprises at least four layers, and a spatial shift of the unit cell does not alter the dispersion curves. However, because the PTBG structure is not infinite long as required by the Bloch's Theorem, the order of layers within each unit cell still might influence the phenomenon of superluminal transmission. To explore this possibility and demonstrate the versatility of achieving superluminal transmission with different values of the parameter δ , Fig. 7 presents two standard TMM simulation results for $\delta = 1.1$. The input pulse is assumed to be a precursor, and two distinct unit cell arrangements, *ABCD* and *CDAB*, are displayed.

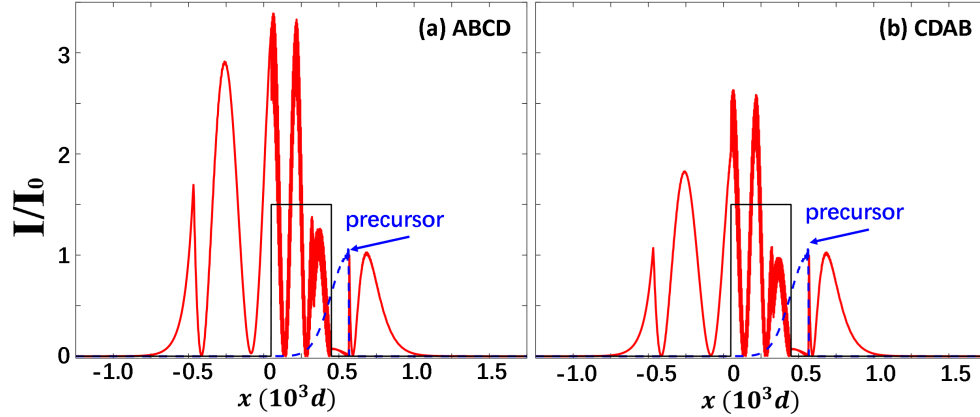


Fig. 7. Distributions of transmitted and reflected pulse for precursors at $\delta = 1.1$ when $t = 1600\tau_0$. The layer sequences are (a) *ABCD* and (b) *CDAB*, respectively.

Figure 7 reveals that the sequence of layers within the unit cell significantly impacts both the transmitted and reflected pulses. However, the observed differences are solely in the field amplitude, without affecting the pulse shape. Importantly, the optical precursors remain consistent with these on the reference. These simulation results provide valuable insights into the phenomenon of superluminal transmission discussed in this article. Firstly, the TMM simulation demonstrates that the superluminal transmission is efficient and achievable within the broken \mathcal{PT} phases with a suitable range of δ . Secondly, the transmission is sensitive to the intricate structure of PTBG materials. However, the superluminal transmission exhibits robustness to the sequence of layers within the unit cell. Thirdly, the optical precursors consistently maintain their luminal nature, that they always propagate at the speed of light c/n_b in the fiber.

The sign of δ also plays a crucial role in regulating the scattering of fields from PTBGs. Figure 8 shows the distributions of transmitted and reflected fields when $\delta = -1.2$ for both the incidence of a Gaussian beam and a precursor. When compared to Figs. 4 and 6, where $\delta = 1.2$, it is evident that although the transmitted fields are independent of the sign of δ , the reflected fields (also the excited fields inside PTBGs) shown in Fig. 8 are significantly diminished compared to those in Figs. 4 and 6. This feature confirms the well-known asymmetric reflection property of \mathcal{PT} systems, which is potentially useful for manipulating the Q factor of resonators for lasing applications [1,2,14–16,19].

Before concluding the numerical analysis, we wish to briefly present the results obtained at EP, which requires setting $\delta = \pm 0.9963$ as indicated in [19]. The simulation results for the incidence of an optical precursor are shown in Fig. 9. The observation delay is set to $t = 2200\tau_0$ to allow sufficient time for the excited field to be efficiently emitted from PTBGs. From Fig. 9, we can see that in both cases, the transmitted pulses overlap perfectly with the reference. Unlike the situations displayed in Figs. 6 and 7, there are no fields preceding the precursors, implying that superluminality does not exist in this scenario. Regarding the reflected components, similar to

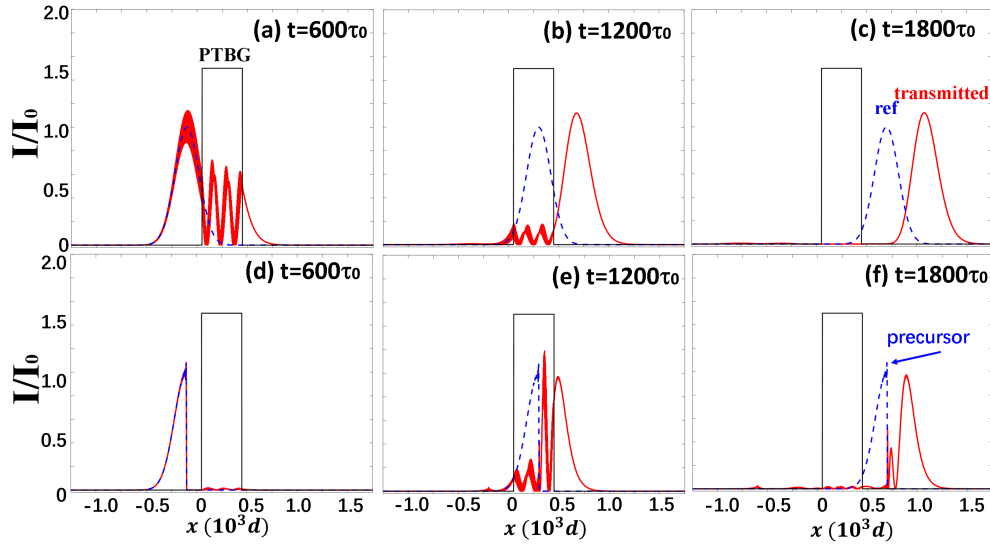


Fig. 8. Distributions of transmitted and reflected fields when $\delta = -1.2$ for the incidence of (a-c) a Gaussian beam and (d-f) a precursor, respectively.

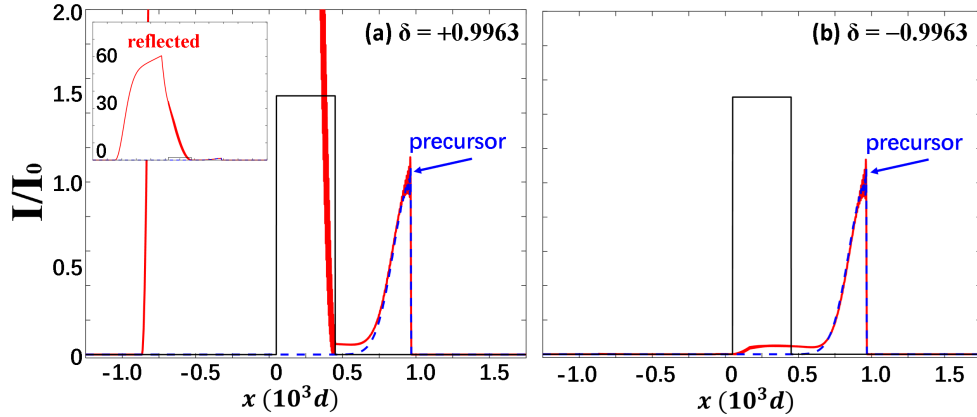


Fig. 9. Distributions of transmitted and reflected fields at EP when $t = 2200\tau_0$. (a) $\delta = 0.9963$ and (b) $\delta = -0.9963$. The inset in (a) shows the global view of I/I_0 .

the asymmetric reflection discussed above, when $\delta = 0.9963$, a very strong reflected pulse is obtained, with the maximum value of I/I_0 exceeding 60. In contrast, when $\delta = -0.9963$, the reflected field is nearly zero. These features are consistent with the collapse of dispersion curves at K_{BZ} [19] and confirm the so-called unidirectional invisibility at EPs [8,9,19].

The study of superluminality in light primarily stems from our scientific curiosity regarding the principle of causality. This phenomenon also holds potential for applications in fields such as telecommunications, information storage, information processing, and interferometry [21]. The theoretical analysis and simulations presented in this article unequivocally demonstrate the existence of efficient superluminal transmission in PTBGs with broken \mathcal{PT} symmetry. These findings confirm the principle of causality in the propagation speed of signals. Moreover, they underscore the immense potential of non-Hermitian physics with broken \mathcal{PT} symmetry, as the transmission coefficient ($T > 1$) observed in this study is significantly higher than that of tunneling ($T \ll 1$). Since the behavior of optical waves can be extended to other harmonic waves, such

as acoustic waves and polaritons, the $T > 1$ superluminality effect can be utilized to manipulate the interactions among waves (or particles) with different group velocities. More specifically, to enhance the interaction among different waves or particles, we could not only employ slow-light techniques to reduce the speed of the fast-propagating waves, but also use the superluminal effect to accelerate those with lower speeds.

The combination of nonlinearity [17,18,35] with superluminality in PTBGs could also lead to numerous attractive applications. However, it is important to emphasize that simulating and analyzing the interaction of optical pulses with nonlinear PTBGs requires the development of novel algorithms beyond the ordinary approaches such as finite-difference time-domain (FDTD) and TMM. FDTD requires artificial techniques to handle gain for different harmonic components in the pulse, and they tend to diverge significantly. The TMM method employed in this article cannot account for the nonlinear contribution because optical nonlinearity is sensitive to local field strength. Addressing this challenge remains an open question for future research. As for experimental validation, to translate our findings into practical reality, we can take advantage of state-of-the-art experimental advancements discussed in numerous influential review articles [1,2,19], particularly those offering insights into design rules for \mathcal{PT} -symmetric gratings operating at 1550 nm [37]. The main challenge in experiments, we believe, is controlling both the spatial distribution and the magnitude of gain.

4. Conclusion

In summary, we show that the dispersion of fiber PTBGs with broken phase supports superluminal light. A light pulse can transmit through a fiber PTBG of broken \mathcal{PT} phase with a high efficient and a preserved Gaussian shape. Such an effect has an obviously advantage over superluminal tunneling where the transmission coefficient is very small. We also discuss the transmission of optical precursors, and show that the precursors cannot be superluminal, in agreement with the principle of causality. This work presents a mechanism for realizing superluminality with some possible applications and underscores the vast potential of non-Hermitian optics.

Funding. National Natural Science Foundation of China (12104203, 12104227, 12274241); Scientific Research Foundation of Nanjing Institute of Technology (YKJ202021); Jiangxi Double-Thousand Plan (jxsq2023101069).

Disclosures. The authors declare no conflicts of interest.

Data availability. Data underlying the results presented in this paper are not publicly available at this time but may be obtained from the authors upon reasonable request.

References

1. L. Feng, R. El-Ganainy, and L. Ge, "Non-Hermitian photonics based on parity-time symmetry," *Nat. Photonics* **11**(12), 752–762 (2017).
2. R. El-Ganainy, K. G. Makris, M. Khajavikhan, *et al.*, "Non-Hermitian physics and \mathcal{PT} symmetry," *Nat. Phys.* **14**(1), 11–19 (2018).
3. S. K. Ozdemir, S. Rotter, F. Nori, *et al.*, "Parity-time symmetry and exceptional points in photonics," *Nat. Mater.* **18**(8), 783–798 (2019).
4. M. A. Miri and A. Alù, "Exceptional points in optics and photonics," *Science* **363**(6422), 42–53 (2019).
5. S. Longhi, "Spectral singularities and Bragg scattering in complex crystals," *Phys. Rev. A* **81**(2), 022102 (2010).
6. K. G. Makris, R. El-Ganainy, D. N. Christodoulides, *et al.*, "Beam dynamics in PT symmetric optical lattices," *Phys. Rev. Lett.* **100**(10), 103904 (2008).
7. M. C. Zheng, D. N. Christodoulides, R. Fleischmann, *et al.*, "PT optical lattices and universality in beam dynamics," *Phys. Rev. A* **82**(1), 010103 (2010).
8. Z. Lin, H. Ramezani, T. Eichelkraut, *et al.*, "Unidirectional invisibility induced by PT-symmetric periodic structures," *Phys. Rev. Lett.* **106**(21), 213901 (2011).
9. A. Mostafazadeh, "Invisibility and PT symmetry," *Phys. Rev. A* **87**(1), 012103 (2013).
10. K. Ding, Z. Q. Zhang, and C. T. Chan, "Coalescence of exceptional points and phase diagrams for one-dimensional PT-symmetric photonic crystals," *Phys. Rev. B* **92**(23), 235310 (2015).
11. E. K. Keshmarzi, R. N. Tait, and P. Berini, "Parity-time symmetry-broken Bragg grating operating with long-range surface plasmon polaritons," *Appl. Phys. A* **122**(4), 279–283 (2016).

12. T. Hao and P. Berini, "Directional coupling with parity-time symmetric Bragg gratings," *Opt. Express* **30**(4), 5167–5176 (2022).
13. P. A. Brandao and S. B. Cavalcanti, "Bragg-induced power oscillations in PT-symmetric periodic photonic structures," *Phys. Rev. A* **96**(5), 053841 (2017).
14. Y. G. Boucher and P. Feron, "Parity-time symmetry in laterally coupled Bragg waveguides," *IEEE J. Quant. Electron.* **55**(6), 1–9 (2019).
15. Z. J. Chen, H. D. Wang, B. Luo, *et al.*, "Parity-time symmetric Bragg structure in atomic vapor," *Opt. Express* **22**(21), 25120 (2014).
16. S. Vignesh Raja, A. Govindarajan, A. Mahalingam, *et al.*, "Tailoring inhomogeneous PT-symmetric fiber-Bragg-grating spectra," *Phys. Rev. A* **101**(3), 033814 (2020).
17. S. Phang, A. Vukovic, H. Susanto, *et al.*, "Impact of dispersive and saturable gain/loss on bistability of nonlinear parity-time Bragg gratings," *Opt. Lett.* **39**(9), 2603–2606 (2014).
18. M. Ali Miri, A. B. Aceves, T. Kottos, *et al.*, "Bragg solitons in nonlinear PT-symmetric periodic potentials," *Phys. Rev. A* **86**(3), 033801 (2012).
19. L. T. Wu, X. Z. Zhang, T. J. Guo, *et al.*, "Superluminality in parity-time symmetric Bragg gratings," *Phys. Scr.* **99**(8), 085544 (2024).
20. L. J. Wang, A. Kuzmich, and A. Dogariu, "Gain-assisted superluminal light propagation," *Nature* **406**(6793), 277–279 (2000).
21. R. W. Boyd and D. J. Gauthier, "Controlling the velocity of light pulses," *Science* **326**(5956), 1074–1077 (2009).
22. H. G. Winful, "Tunneling time, the Hartman effect, and superluminality: a proposed resolution of an old paradox," *Phys. Rep.* **436**(1-2), 1–69 (2006).
23. S. Longhi, M. Marano, P. Laporta, *et al.*, "Superluminal optical pulse propagation at 1.5 μm in periodic fiber Bragg gratings," *Phys. Rev. E* **64**(5), 055602 (2001).
24. G. D'Aguanno, M. Centini, M. Scalora, *et al.*, "Group velocity, energy velocity, and superluminal propagation in finite photonic band-gap structures," *Phys. Rev. E* **63**(3), 036610 (2001).
25. A. M. Steinberg and R. Y. Chiao, "Subfemtosecond determination of transmission delay times for a dielectric mirror (photonic band gap) as a function of the angle of incidence," *Phys. Rev. A* **51**(5), 3525–3528 (1995).
26. Ch. Spielmann, R. Szipocs, A. Stingl, *et al.*, "Tunneling of optical pulses through photonic band gaps," *Phys. Rev. Lett.* **73**(17), 2308–2311 (1994).
27. T. E. Hartman, "Tunneling of a wave packet," *J. Appl. Phys.* **33**(12), 3427–3433 (1962).
28. D. J. Gauthier and R. W. Boyd, "Fast light, slow light and optical precursors: what does it all mean?" *Photonics Spectra* **41**(1), 82–90 (2007).
29. H. Jeong, A. M. C. Dawes, and D. J. Gauthier, "Direct observation of optical precursors in a region of anomalous dispersion," *Phys. Rev. Lett.* **96**(14), 143901 (2006).
30. S. Zhang, J. F. Chen, C. Liu, *et al.*, "Optical precursor of a single photon," *Phys. Rev. Lett.* **106**(24), 243602 (2011).
31. L. Ge and H. E. Tureci, "Antisymmetric \mathcal{PT} -photonic structures with balanced positive- and negative-index materials," *Phys. Rev. A* **88**(5), 053810 (2013).
32. Y. Choi, C. Hahn, J. W. Yoon, *et al.*, "Observation of an anti- \mathcal{PT} -symmetric exceptional point and energy-difference conserving dynamics in electrical circuit resonators," *Nat. Commun.* **9**(1), 2182–2187 (2018).
33. L. T. Wu, X. Z. Zhang, R. Z. Luo, *et al.*, "Non-Hermitian guided modes and exceptional points using loss-free negative-index materials," *Opt. Express* **31**(9), 14109–14118 (2023).
34. A. M. Jazayeri, "Fixed points on band structures of non-Hermitian models: extended states in the bandgap and ideal superluminal tunneling," *Phys. Rev. B* **107**(14), 144302 (2023).
35. Y. Pan, M. I. Cohen, and M. Segev, "Superluminal k-gap solitons in nonlinear photonic time crystals," *Phys. Rev. Lett.* **130**(23), 233801 (2023).
36. J. B. Khurgin and R. S. Tucker, *Slow Light: Science and Applications* (CRC Press, 2018), pp. 293–320.
37. H. Benisty, V. B. de la Perriere, A. Ramdane, *et al.*, "Parity-time symmetric gratings in 1550 nm distributed-feedback laser diodes: insight on device design rules," *J. Opt. Soc. Am. B* **38**(9), C168–c174 (2021).